

RELATIVISTIC THEORY FOR LASER-ION ACCELERATION*

Y. S. Huang, N. Y. Wang, X. Z. Tang, Y. J. Shi

High Power Excimer Laser Laboratory, China Institute of Atomic Energy, 102413, China

Abstract

An analytical relativistic model is proposed to describe the relativistic ion acceleration in the interaction of ultra-intense laser pulses with thin-foil plasmas. It is found that there is a critical value of the ion momentum to make sure that the ions are trapped by the light sail and accelerated in the radiation pressure acceleration (RPA) region. If the initial ion momentum is smaller than the critical value, that is in the classical case of RPA, the potential has a deep well and traps the ions to be accelerated. There is a new ion acceleration region different from RPA, called ultra-relativistic acceleration, if the ion momentum exceeds the critical value. In this case, ions will experience a potential downhill. The dependence of the ion momentum and the self-similar variable at the ion front on the acceleration time has been obtained. The critical conditions of the laser and plasma parameters which identify the two acceleration modes have been achieved. No matter RPA or ultra-relativistic acceleration, the potential difference is a constant, which dedicates the maximum ion energy.

INTRODUCTION

As a promising method to generate relativistic mono-energetic protons, radiation pressure acceleration (RPA) attracts more and more attentions[1, 2, 3, 4, 5, 6] and becomes dominant in the interaction of the ultra-intense laser pulse with nanometer foils. When an ultra-short and ultra-intense laser pulse is shot on a thin foil, the foil is ionized immediately. At the same time, the electrons obtain relativistic velocity and move forward. The ions are accelerated by the strong separation field between the ions and electrons. Simultaneously, the electrons are pulled back and form recirculation around the ions and accumulate locally. The local potential is smaller than that at the boundary due to the accumulation of the electrons, therefore a well forms at the position of the ion shell. When the laser exists, the electrons obtain energy continuously to maintain the temperature and the high-density distribution. Therefore, the potential well maintains and traps ions in the time period. The high-density electron shell is compared to a light sail(LS)[6]. In LS[5, 6] model, the charge-separation field between the ions and the electron shell accelerates the ions trapped in the potential well[3, 4, 5], which is generated by the electron recirculation from the electron shell. Eliasson and coworkers[4] solved the relativistic ion mo-

mentum equation ignoring the collective effect of plasmas and discussed the condition of the radiation pressure compared with the electrostatic force to avoid the total separation of ions and electrons. The integration of the electron field along the longitudinal axis shows the electric potential well, as shown by Figure 2 (c), 3 (c), and 6(c) in simulations[4], which traps some ions. The velocity of the trapped ions is close to that of the well, and of course, there is a critical value of it to avoid the trapped ions escape from the well. However, without considering the collective effect of the plasma, they did not deduce the potential well and the critical velocity of the trapped ions analytically. Yan and coworkers tried to predict the ion energy distribution with a self-similar hydrodynamic theory[7]. However, it is nonrelativistic with the plasma approximation which allows $\nabla \cdot E \neq 0$ and $n_i - n_e = 0$ simultaneously, where E is the acceleration field and n_i (n_e) is the ion (electron) density. Therefore, the critical velocity of the trapped ion in the potential well was not given.

An analytical solution of the relativistic hydrodynamical system is obtained under the assumption of self-similar state and density distribution. We set an expression for the critical ion momentum, which divides the relativistic ion acceleration into two modes. One is nothing but the classical RPA described before in which the ion momentum is lower than the critical one. The other is newly identified by ours, called ultra-relativistic acceleration (URA). In the ultra-relativistic limit, the maximum ion momentum at the ion front is proportional to $t^{4/5}$, where t is the acceleration time.

BASIC ASSUMPTIONS, RELATIVISTIC EQUATIONS AND AN ANALYTICAL RELATIVISTIC SOLUTION

For convenience, the physical parameters: the time, t , the ion position, x , the ion velocity, v , the electron field, E , the electric potential, φ , the plasma density, n , and the light speed, c , are normalized by ω is the light frequency, $k = \omega/c$ is the wave number, c is the light speed, $E_0 = k\varphi_0$, and n_0 is the reference density, respectively, where $e\varphi_0 = \gamma_{em}m_e c^2$ and γ_{em} is the maximum electron energy. Here e is the elemental charge.

With reference to the results given by Mako and Tajima in Ref. [7], in the self-similar state, the density distribution of ions is assumed to be:

$$\hat{n}_k = \frac{1}{\Sigma Q_k} (1 + \phi)^\alpha, k = 1, \dots, N \quad (1)$$

where the subscript k stands for the ion species, Q_k is the charge number of the k th species ion, the index α depends

*Work supported by the Key Project of Chinese National Programs for Fundamental Research (973 Program) under contract No. 2011CB808104 and the Chinese National Natural Science Foundation under contract No. 10834008 and No. 11105233.

on the laser intensity and the target thickness and has been discussed in Ref. [7].

With the transformation: $\xi = \hat{x}/\tau$, the normalized continuity and motion equation of ions are given as:

$$(u_k - \xi) \frac{\partial \ln \hat{n}_k}{\partial \xi} = -\frac{\partial u_k}{\partial \xi} \quad (2)$$

$$(u_k - \xi) \frac{\partial \gamma_k u_k}{\partial \xi} = -\mu_k \frac{\partial \phi}{\partial \xi} \quad (3)$$

where $\mu_k = \frac{Q_k \gamma_{em} m_e}{M_k}$, M_k is the mass of certain ion, $\gamma_k = (1 - u_k^2)^{-1/2}$.

Therefore, the potential is acquired as a function of ξ and u_k :

$$1 + \phi = \frac{\alpha}{\mu_k} (u_k - \xi)^2 \gamma_k^3 \quad (4)$$

or:

$$u_k - \xi = \pm \sqrt{\frac{\mu_k}{\alpha}} \sqrt{1 + \phi} \gamma_k^{-3/2} \quad (5)$$

where '+' corresponds to $u_k \geq \xi$ and '-' corresponds to $u_k \leq \xi$.

With Equation (4), the initial conditions are not arbitrarily taken and satisfy following relation:

$$1 + \phi_0 = \frac{\alpha}{\mu_k} (u_{k,0} - \xi_0)^2 \gamma_{k,0}^3 \quad (6)$$

where $\xi_0 = \xi(u_k = u_{k,0})$ and $\gamma_{k,0} = (1 - u_{k,0}^2)^{-1/2}$.

Therefore, the normalized potential in the ion region satisfies:

$$\phi = \frac{(\chi - \chi_0 - 2\alpha(u_{k,0} - \xi_0)\gamma_{k,0}^{3/2})^2}{4\alpha\mu_k} - 1 \quad (7)$$

where $\chi_0 = \chi(u_{k,0})$, $\chi = \int_0^{u_k} \gamma_k^{3/2} du_k$. In the ultra-relativistic limit that $u_k \rightarrow 1$, the potential tends to the constant:

$$\lim_{u_k \rightarrow 1} \phi \hat{=} \phi_\infty = \frac{(\chi_\infty - \chi_0 - 2\alpha(u_{k,0} - \xi_0)\gamma_{k,0}^{3/2})^2}{4\alpha\mu_k} - 1 \quad (8)$$

Combining Eqs. (5) and (6), the dependence of the normalized ion velocity on the self-similar variable is given by:

$$\xi = u_k + \frac{\gamma_k^{-3/2}}{2\alpha} (\chi - \chi_0) - (u_{k,0} - \xi_0) \left(\frac{\gamma_{k,0}}{\gamma_k} \right)^{3/2} \quad (9)$$

With Eqs. (1) and (7), the self-similar density distribution satisfies:

$$\hat{n}_k = \left[\frac{(\chi - \chi_0 - 2\alpha(u_{k,0} - \xi_0)\gamma_{k,0}^{3/2})^2}{4\alpha\mu_k} \right]^\alpha \quad (10)$$

Until now, the analytical solution for the self-similar state has been achieved as shown by Eqs. (7), (9) and (10).

As shown by Figure 1 (a), the results of our model are consistent with that of the thin-shell model and PIC simulations[1].

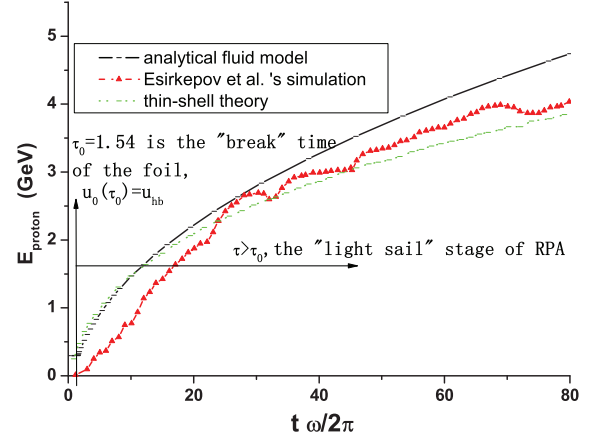


Figure 1: (Color online) Comparison of our analytical model with thin-shell model and Esirkepov et al.'s simulations for $\sigma/a \approx 0.1$, $a = 316$, $d = \lambda = 1\mu\text{m}$, $n_0 = 49n_c = 5.5 \times 10^{22}/\text{cm}^3$, and $\alpha = 1.8$ [7].

TWO ACCELERATION MODES

Being different from the nonrelativistic case[7], there are two distinct acceleration modes depending on the initial conditions: $u_{k,0}$, ξ_0 and α in the relativistic case.

Here we set a critical value for ion momentum from the following condition:

$$\chi_\infty - \chi_c - 2\alpha(u_{k,c} - \xi_0)\gamma_{k,c}^{3/2} = 0 \quad (11)$$

where $\chi_c = \chi(u_{k,c})$ and $p_{k,c} = \gamma_{k,c}u_{k,c}$. Figure 1(b) shows the critical phase space for a series of α .

In the following discussion, it is assumed $\xi_0 = 0$ and $\alpha = 2$ to reveal the physical mechanisms of relativistic RPA for different conditions.

In the following calculations, with Eqs. (7), (9) and (10), the plasma density, the potential and the self-similar parameter, ξ are all deemed to be functions of the ion momentum. Therefore, the dependence of the plasma parameters and field on ξ can be obtained for different conditions.

(A) RPA under the condition: $p_{k,0} < p_{k,c}$ given by Eq. (11), that is for example, $p_{k,0} < 0.5064$ at $\xi_0 = 0$ and $\alpha = 2$.

In this case, the ion velocity is not large enough to escape from the potential well formed by the electron shell, which was described by Eliasson and coworkers[4]' simulations. The potential well and the acceleration field have been deduced here analytically in detail and shown by Figure 3 (b)[8], which supports the simulation results[4].

The potential well is formed by the electron shell and can trap ions and accelerate them and suppress their energy dispersion. However the ion energy distribution is not monoenergetic. It is consistent with the results shown by the long-time simulations[2, 9, 10] and the experimental detections[2, 10].

In this case, RPA is divided into two regions theoretically: the phase-stable acceleration region (PSA) for $0 \leq \xi \leq \xi_{i,f}$ and the phase-stable deceleration region (PSD) $\xi_{i,f} \leq \xi \leq 1$.

(I) In PSA region, $0 \leq \xi \leq \xi_{i,f}$, the electric field $E \geq 0$ and the electron density is larger than the ion density.

The potential shown by Figure 3[8] in $0 \leq \xi \leq \xi_{i,f}$ gives a physical explanation of PSA for $a_0 = 70, n_0 = 49n_c$. The ions coast down with the slope of the potential, and the gradient, i.e., the electric field, becomes weaker as the ions come to the bottom of the potential. The ions at higher potential will obtain more acceleration, therefore the energy spread is suppressed. Different from the real gliding process, the ions cannot pass through the bottom and climb up since the ion front is the limiting point with the ion density tending to zero there.

(II) In PSD region, $\xi_{i,f} \leq \xi \leq 1$, the electric field $E \leq 0$ and the electron density is larger than the ion density too as shown in Figure 3[8]. Similar to the special case for $\phi_0 = -1$, this region is also a non-physical region for ion acceleration.

Combining the above discussion about PSA and PSD, the ions with an initial momentum of $p_{k,0}$, which is not large enough to get across the potential at $\xi = 1$, are trapped in PSA region or PSD region and obtain a finite maximum energy at the ion front $\xi_{i,f} < 1$. Therefore, it is in the RPA region.

(B) URA for $p_{k,0} > p_{k,c}$ given by Eq. (11), that is for example $p_{k,0} \geq 0.5064$ at $\xi_0 = 0$ and $\alpha = 2$.

$$\int_0^{p_{k,0}} \gamma_k^{-\frac{3}{2}} dp_k + 2\alpha(p_{k,0} - \gamma_{k,0}\xi_0)\gamma_{k,0}^{\frac{1}{2}} \geq \chi_\infty \quad (12)$$

for $p_{k,0} \geq 0.5064$, i.e., $a_0 \geq 143$ for protons, the ions will coast down with the potential slope and drop into the bottomless abyss at $\xi = 1$ as shown by Figure 4[8].

In the ultra-relativistic limit, combining Eqs. (9) and (8), it is found that:

$$\frac{\partial^2 \phi}{\partial \xi^2} \propto -\gamma_k^{5/2}, \gamma_k \gg 1 \quad (13)$$

The ion momentum at the ion front satisfies:

$$\gamma_{i,f} \approx p_{i,f} \propto \tau^{4/5} \quad (14)$$

for $p_{i,f} \gg 1$.

Equation (14) shows the dependence of maximum ion energy at the ion front on the acceleration time in the ultra-relativistic limit. It cannot be compared with the results in Figure 1 because they correspond to different physical situations. Equation (14) is satisfied in the ultra-relativistic limit, i.e., $p_{i,f} \gg 1$, and shows that the maximum ion energy at the ion front is proportional to $\tau^{4/5}$. However, the results shown in Figure 1 are neither for the ultra-relativistic limit nor for the maximum ion energy at the ion front. It is shown that the average ion energy when the relativistic factor is not far larger than unit. The ions at the ion front can be accelerated more efficiently since the field there is the most intense and the field behind the ion front is shielded by the ions beyond them.

LIMIT FOR THE MAXIMUM ION ENERGY

No matter in the RPA region or in the ultra-relativistic acceleration region, the maximum ion energy is limited by the potential difference:

$$E_{m,i} \leq \Delta\phi = \phi_\infty - \phi_0 \quad (15)$$

CONCLUSION

Under the assumptions of the ion density distribution of Eq. (1) and self-similar state, an analytical relativistic solution of the hydrodynamic equations and Poisson's equation is obtained which describe the relativistic ion acceleration consistently. Depending on laser intensity and the surface density of the plasma, the ion momentum determines two distinctive acceleration modes: the classical relativistic RPA and ultra-relativistic acceleration which is newly identified.

REFERENCES

- [1] T. Esirkepov, M. Borghesi, S. V. Bulanov, G. Mourou, and T. Tajima, Phys. Rev. Lett. 92, 175003 (2004).
- [2] A. Henig, S. Steinke, M. Schurrer, et al., Phys. Rev. Lett. 103, 245003 (2009).
- [3] X. Q. Yan, C. Lin, Z.M. Sheng, et al., Phys. Rev. Lett. 100, 135003 (2008).
- [4] B. Eliasson, C. S. Liu, X. Shao, R. Z. Sagdeev and P. K. Shukla, New J. Phys. 11, 073006 (2009).
- [5] A. Macchi, S. Veghini, T. V. Liseykina and F. Pegoraro, New J. Phys. 12, 045013 (2010).
- [6] B. Qiao, M. Zepf, M. Borghesi, B. Dromey, M. Geissler, A. Karmakar and P. Gibbon, Phys. Rev. Lett., 105, 155002 (2010).
- [7] X. Q. Yan, T. Tajima, M. Hegelich, et al., Appl. Phys. B, 98, 711-721 (2010).
- [8] Y. S. Huang, N. Y. Wang, X. Z. Tang, Y. J. Shi, and X. Q. Yan, Physics of Plasmas 19, 093109 (2012).
- [9] H. B. Zhuo, Z. L. Chen, W. Yu, Z. M. Sheng, M. Y. Yu, Z. Jin, and R. Kodama, Phys. Rev. Lett. 105, 065003 (2010).
- [10] D. Jung, L. Yin, B. J. Albright, D. C. Gautier, R. Horlein, D. Kiefer, A. Henig, R. Johnson, S. Letzring, S. Palaniyappan, R. Shah, T. Shimada, X. Q. Yan, K. J. Bowers, T. Tajima, J. C. Fernandez, D. Habs, and B. M. Hegelich, Phys. Rev. Lett. 107, 115002 (2011).